

Sprayed Oil–Water Microdroplets as a Hydrogen Source

Xuke Chen,^{||} Yu Xia,^{||} Yingfeng Wu,^{||} Yunpeng Xu, Xiuquan Jia,* Richard N. Zare,* and Feng Wang*



Cite This: *J. Am. Chem. Soc.* 2024, 146, 10868–10874



Read Online

ACCESS |



Metrics & More

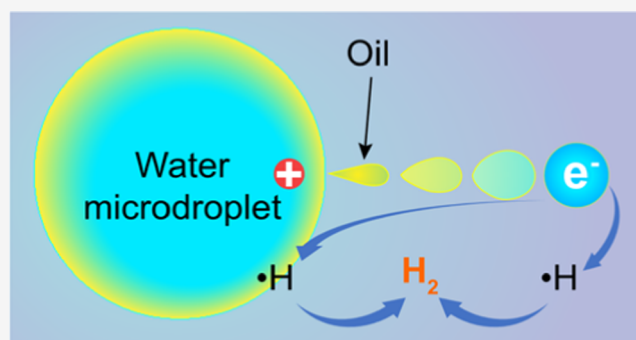


Article Recommendations



Supporting Information

ABSTRACT: Liquid water provides the largest hydrogen reservoir on the earth's surface. Direct utilization of water as a source of hydrogen atoms and molecules is fundamental to the evolution of the ecosystem and industry. However, liquid water is an unfavorable electron donor for forming these hydrogen species owing to its redox inertness. We report oil-mediated electron extraction from water microdroplets, which is easily achieved by ultrasonically spraying an oil–water emulsion. Based on charge measurement and electron paramagnetic resonance spectroscopy, contact electrification between oil and a water microdroplet is demonstrated to be the origin of electron extraction from water molecules. This contact electrification results in enhanced charge separation and subsequent mutual neutralization, which enables a ~13-fold increase of charge carriers in comparison with an ultrapure water spray, leading to a ~16-fold increase of spray-sourced hydrogen that can hydrogenate CO₂ to selectively produce CO. These findings emphasize the potential of charge separation enabled by spraying an emulsion of liquid water and a hydrophobic liquid in driving hydrogenation reactions.



INTRODUCTION

The hydrogen atom ($\bullet\text{H}$) and molecule (H_2) play a key role in the evolution of earth^{1,2} and life,^{3,4} in human health and disease,^{5,6} and in the pursuit of net-zero carbon emission.^{7–10} Yet, most hydrogen on the earth is oxidized and held in the form of water. Liquid water is very redox-inert owing to the high adiabatic ionization potential (AIP of $\text{OH}^- = 6.1$ eV based on photoelectron spectrum results and values for absolute solvation free energies) of OH^- to form $\bullet\text{OH}$ ¹¹ and the high thermodynamic potential (1.23 V) required to split water into H_2 and O_2 , making it a formidable challenge to use water as the source of reduced hydrogen.⁷ Unlike inert bulk-phase water, water microdroplets have been shown in many studies to possess a high electric field at the interface of microdroplets,^{12–15} which is sufficient to spontaneously ionize OH^- to produce free electrons.^{16–21} Recent studies show that subsequent charge transfer can lead to a variety of essential hydrogenation reactions under ambient conditions,^{22–28} such as the fixation of N_2 to ammonia and urea,^{24,28} fixation of CO_2 by the reverse tricarboxylic acid cycle,²⁶ and formation of formic acid from CO_2 .^{19,22,27} Utilization of water microdroplets as a hydrogen source for selective hydrogenation has the potential to rapidly arouse intense interest in a variety of fields ranging from ecosystem remediation to best industrial practice, given that water microdroplets and water are ubiquitous on the earth's surface. It is therefore important to determine the drivers of the hydrogen evolution reaction at the microdroplet interface.

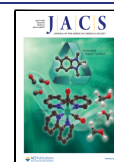
Charge separation is a fundamental step in nearly all chemical processes that occur at interfaces. As early as 1892, Lenard noticed that when water breaks into tiny droplets, the negative and positive charges are separated,^{29,30} which is the earliest indication of water microdroplet-mediated charge separation. It was recently proposed that this is a size-dependent charge separation driven by a propensity of interfacial negative charges moving from large microdroplets to small microdroplets.^{31,32} Subsequent mutual neutralization of separated hydrated ions with opposite charges is a very fundamental chemical reaction that can exhibit a rich variety of products.³³ In merged beams of hydronium and hydroxide, the released kinetic energy by mutual neutralization can ignite electron transfer³⁴ and was recently found to be capable of driving a formation of $\bullet\text{H}$ and H_2 product from water.³³ However, the chemical impact of mutual neutralization over charged water microdroplets on such hydrogen species' formation is poorly understood. In terms of water microdroplets, the water–gas interface is only ~2 solvation layers (<0.35 nm) thick,³⁵ providing an extremely limited space for charge carrier separation and neutralization. Therefore, a comparative study of sprayed water microdroplets with

Received: January 30, 2024

Revised: March 4, 2024

Accepted: March 20, 2024

Published: April 4, 2024



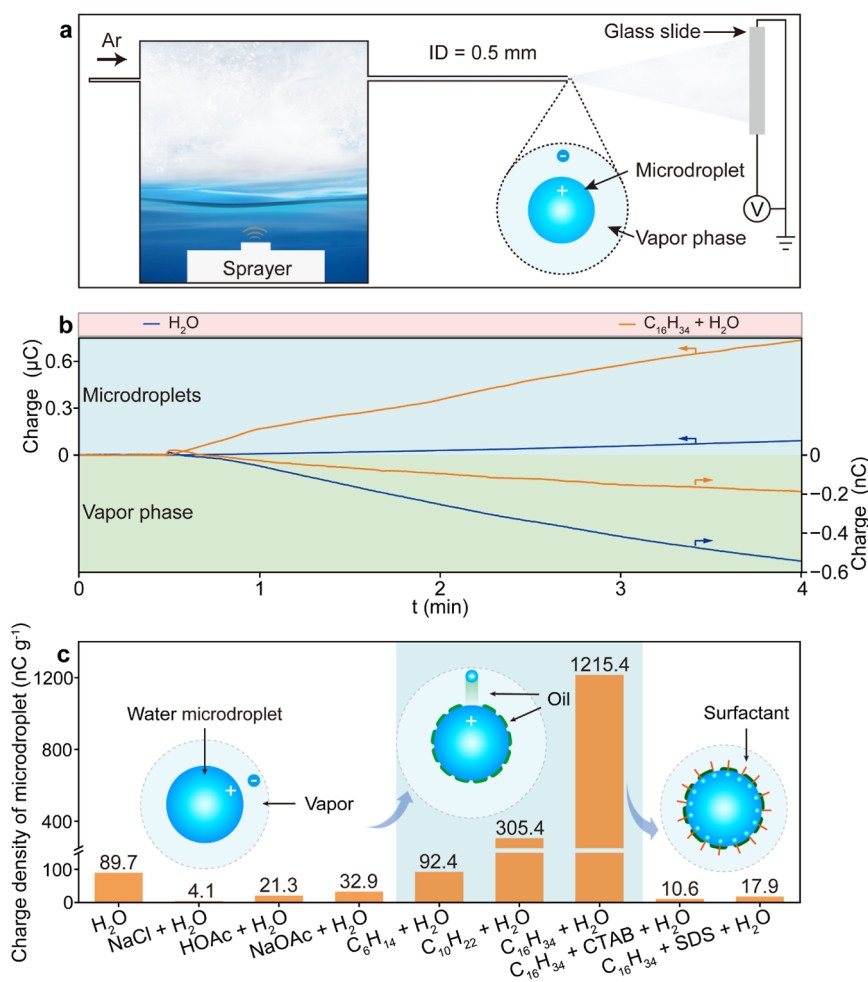


Figure 1. Sprayed hexadecane–water microdroplets and vapor phase. (a) Experimental setup. (b) Charge measurements of microdroplets and the vapor phase. (c) Measured electric charge density of microdroplets with additives.

thickening interfacial charge layers should be a promising way to understand the cause-and-effect relationship between charge transfer and hydrogenation reactions employing sprayed water microdroplets.

The oil–water interface has a >1 nm aqueous layer that has charge density oscillations as well as a ~ 0.5 nm thick oil phase that are loaded with delocalized electrons.³⁶ Our previous study has shown the ability of the oil–water microdroplet interface to produce hydrogen atoms ($\cdot\text{H}$) and molecular hydrogen (H_2) via water-to-oil charge transfer.²⁵ In this study, we observed that when an oil–water mixture is sprayed, contact electrification between oil and water can be employed to extract electrons from the sprayed microdroplets. This results in a ~ 13 -fold increase of charge carriers in comparison with an ultrapure water spray. The enhanced charge separation gives an improvement of a factor of ~ 16 in the spray-sourced hydrogen evolution from water, which is verified to possess reducing capacity to selectively hydrogenate CO_2 to form CO .

RESULTS

Charge Measurement of Microdroplets and the Vapor Phase. Sprayed oil–water microdroplets were prepared by ultrasonically atomizing a mixture of 0.5 mL of hexadecane and 70 mL of water (Figures 1a and S1). The spray electrification of microdroplets can be investigated by measuring the accumulated charge of microdroplets collected

on a nonconductive glass slide with an electrometer, as shown in Figure 1a. The spray electrification of the vapor phase was probed by trapping the microdroplets in a second quartz reactor to allow for the vapor phase to be exported separately to the glass slide, as shown in Figure S2. Figure 1b shows the charge of microdroplets and the surrounding vapor phase generated during ultrasonic atomization of both ultrapure water and a hexadecane–water emulsion. The microdroplets tended to carry positive charges while the vapor phase tended to be negatively charged. Compared to the positive charge of microdroplets, the negative charge of the vapor phase was reduced by 3 orders of magnitude. We speculate that the majority of the negatively charged particles in the vapor phase did not reach the glass slide but remained in the second reactor or escaped with the leaking gas without contacting the glass slide. When hexadecane was added, the positive charge of the resulting microdroplets markedly increased, with the charge per unit mass of oil–water microdroplets being ~ 13 times larger than that of ultrapure water microdroplets (Figure 1c), whereas the negative charge of the ultrapure water vapor phase exceeded that of the oil–water vapor phase (Figure 1b). This behavior might be attributed to the fact that the negative charge carriers are dominated by oil molecules, which have a propensity for deposition and have a relatively short residence time in the gas phase in comparison with the water vapor.

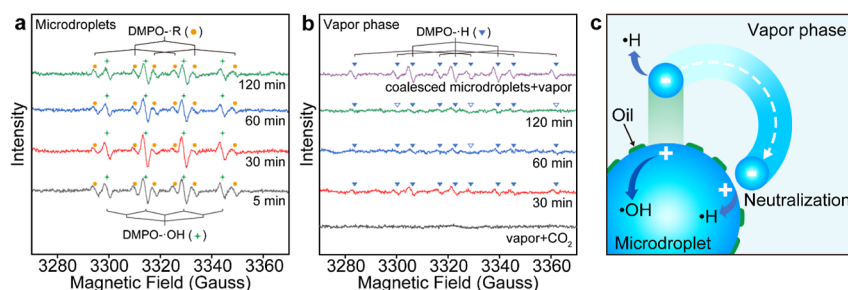


Figure 2. Observation of radicals formed in an ultrasonic spray as detected by EPR spectroscopy in (a) microdroplets and the (b) vapor phase. (c) Schematic diagram of the mechanism for radical formation.

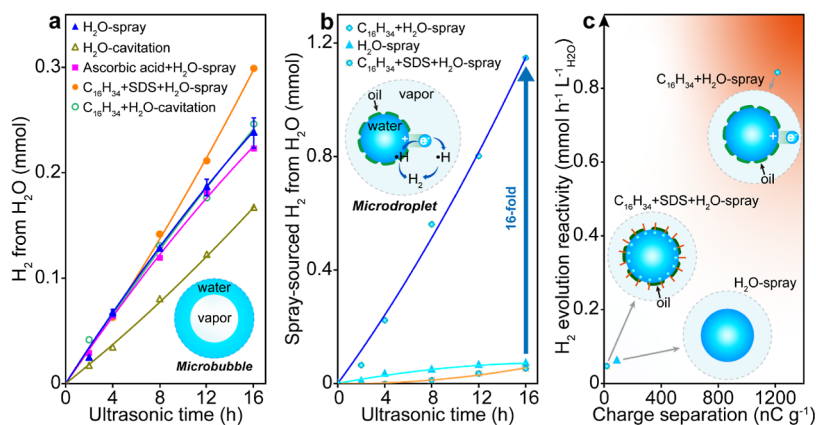


Figure 3. Evolution of H_2 . (a) Time courses of the H_2 product generated by water spray and by water cavitation. (b) Comparison of a spray-sourced H_2 product generated from water in spraying a hexadecane–water solution, a hexadecane–SDS–water solution, and ultrapure water. (c) Relationship between charge separation of microdroplets and spray-sourced H_2 evolution reactivity. The atomizer was placed in a sideways direction in the case of cavitation only.

To clarify further the relationship between the oil and the charge of microdroplets, various ionizable additives, including sodium chloride, sodium acetate, and acetic acid, were also dissolved in water microdroplets and sprayed (Figure 1c). It is noteworthy that among these additives, only oil resulted in a substantial enhancement in the electrification of the sprayed microdroplets. Therefore, the contact electrification between oil and water is mainly a result of electron transfer from water to oil rather than ionic migration. The introduction of ionic additives has been found to account for an enhanced interfacial electric field owing to the spatial separation of anions and cations that tend to accumulate at the surface of individual microdroplets.^{37,38} On the other hand, this would also result in a reduction of the electric double-layer thickness,³⁹ thereby constraining the space for charge carrier transportation. The charge separation in oil–water systems was enhanced as the volatility of alkanes decreased (Figure 1c). Furthermore, the addition of surfactants such as hexadecyl trimethylammonium bromide (CTAB), sodium dodecyl sulfonate (SDS), and nonionic surfactants to occupy the interfacial region resulted in the accumulation of oil on the surface of water droplets (Figure S3) and a significant reduction in the charge of microdroplets (Figures 1c and S4). Additionally, as particle size significantly influences properties of microdroplets, such as pH and ion distribution,^{40,41} we measured the size distribution of microdroplets generated from the atomization of oil–water systems (Figure S5). The results indicate that the diameters of sprayed microdroplets in the hexadecane–water system are primarily in the range of 2–5 μm , and the addition of surfactants caused a slight narrowing of the size distribution of microdroplets. The

results presented above provide compelling evidence for a positive correlation between the oil–water interfaces and the electrification of sprayed oil–water emulsion microdroplets. This behavior might be related to our previously reported phenomenon that oil molecules are spontaneously separated from the surface of oil–water emulsion microdroplets during the fragmentation and contraction of water,²⁵ which should enhance the charge separation initiated by the contact electrification between oil and water.

Separate Distributions of Reducing and Oxidizing Free Radicals. Next, we attempted to verify the chemical consequence of charge transfer by probing the evolution of radicals with EPR spectroscopy using 5,5-dimethyl-1-pyrroline *N*-oxide (DMPO) as a probe (Figure 2). The radicals in microdroplets were investigated after exporting the microdroplets into the liquid nitrogen cold trap charged with DMPO under an Ar atmosphere. In Figure 2a, EPR quadruplet DMPO– $\bullet\text{OH}$ peaks and sextet DMPO– $\bullet\text{R}$ peaks were observed in the exported hexadecane–water microdroplets which were positively charged. It implies that the extraction of electrons from microdroplets led to the formation of electron-deficient hydroxyl radicals ($\bullet\text{OH}$), which further resulted in the generation of hydrocarbon free radicals ($\bullet\text{R}$). Considering the formation of $\bullet\text{R}$, it raised the question of whether hexadecane might potentially serve as a sacrificial electron donor in the charge-transfer process. Further experiments and discussions were conducted to investigate this possibility (Figure 3a).

The chemical fate of electrons extracted from microdroplets via contact electrification could be inferred from the EPR signals of the negatively charged vapor phase. Upon trapping

the exported microdroplets, the appearance of radicals exhibiting EPR nonuple DMPO- \bullet H peaks in the remanent carrier gas (Figure 2b) indicated the formation of hydrogen radicals (\bullet H). In addition, no signals of DMPO- \bullet R were observed in the vapor phase, demonstrating that \bullet H was not generated by hydrogen abstraction from oil. Subsequently, with the accumulation of coalesced microdroplets and vapor in the trap, the intensity of vapor-phase \bullet H-derived signals decreased. Notably, strong DMPO- \bullet H peaks appeared instead of DMPO- \bullet OH peaks in the bulk phase deriving from the coalescence of microdroplets and the vapor phase, indicating the generation of \bullet H during the coalescence. This should result from the neutralization mechanisms existing between the positively charged microdroplets and negatively charged vapor in the chemical environment of ultrasonic atomization, which can lead to the generation of excess energy. When separated water ions with opposite charges collide and neutralize mutually, the excess energy of up to 9.78 eV⁴² may facilitate the fragmentation of H₂O at water microdroplet interfaces, leading to the formation of neutral hydrated hydrogen radicals.³³ This results in a higher intensity of hydrogen radical signals in the coalesced phase compared to the vapor phase. Moreover, the signals of DMPO- \bullet H in the vapor phase disappeared when CO₂ was introduced into the vapor phase, suggesting that \bullet H was being removed by reaction with CO₂. These results revealed that contact electrification between oil and water involved the oil-mediated extraction of electrons from sprayed microdroplets, which could subsequently provide active hydrogen species (Figure 2c).

Evolution of H₂ by Sprayed Water Microdroplets. We next explored the H₂ evolution reactivity of two different systems, either by water spraying into microdroplets or by water cavitation into microbubbles. To quantify the amount of H₂ generated from water in oil-containing systems, we used the H/D ratio of 0.282 observed in the atomization of the hexadecane-D₂O system as a reference for quantifying the H₂ generated from water. The H₂ derived from water should account for 78% of the total H₂ production (Figure S6). Figure 3a shows the time course of H₂ generated under different spraying conditions. In the ultrasonic spray process, H₂ can originate from both spray and cavitation. In terms of ultrapure water, the H₂ generated by ultrasonic spray is just slightly higher than that in the absence of spray, indicating that cavitation is the primary origin of H₂ in the ultrasonic spraying of ultrapure water. Likewise, the H₂ generated by ultrasonic spray of the hexadecane-SDS-water system is also predominantly derived from cavitation, which is just slightly higher than that in the case of ultrapure water, while the spray-sourced H₂ product generated from water within 16 h from a hexadecane-SDS-water solution is less than that in pure water (Figure 3b). Therefore, when charge separation is limited (Figure 1c), ultrasonically sprayed aqueous microdroplets are much less active for generating H₂ than cavitation-based microbubbles.

In comparison with the ultrasonically sprayed ultrapure water, about a 16-fold increase of the efficiency of spray-sourced hydrogen evolution from water was observed in the hexadecane-water emulsion system (Figure 3b), coinciding with the \sim 13-fold enhancement of charge separation (Figure 1c). Thus, H₂ generated by the ultrasonic spray of an oil-water emulsion becomes predominantly spray-sourced (Figure S7). These results demonstrate that the spray-sourced H₂ evolution reactivity is positively correlated with the charge

separation efficiency which varies by adjusting the thickness of the charge layer at a microdroplet interface (Figure 3c). The addition of ascorbic acid which acts as both a reactive oxygen species (ROS) scavenger and a sacrificial electron donor did not improve H₂ formation (Figure 3a). This result suggests that ROS removal and additional supply of a sacrificial electron donor are not the origin of the enhanced H₂ formation kinetics in the ultrasonic water spray process. A kinetic isotope effect of 2.32 in the generated H₂ was observed upon replacing H₂O with D₂O (Figure S8), indicating that water autoionization is the kinetically relevant step. In addition, the oil failed to be atomized in the absence of water, and no H₂ was generated, although a minor generation of H₂ was observed when there was a small amount of water and an excess of oil, despite the lack of observable atomization (Figure S9). This result indicates that H₂ generation from oil is challenging under high-frequency ultrasonic irradiation and cannot occur directly. It requires prior oxidation to generate water, followed by H₂ generation from the water. Thus, the electron donor of spray-sourced hydrogen (\bullet H and H₂) should directly come from the electron transfer of OH⁻, whose concentration is limited by the water autoionization. To sum up, although the inherent H₂ formation activity of sprayed ultrapure water microdroplets is relatively low, the addition of oil does significantly enhance the activity. And the charge separation of sprayed microdroplets enabled by the contact electrification at the oil-water interface of a microdroplet plays the key role in promoting H₂ generation.

In Situ CO₂ Hydrogenation over Sprayed Oil-Water Microdroplets for CO Formation. To experimentally validate the hydrogen reactivity, ultrasonic spray-mediated CO₂ hydrogenation was investigated. As shown in Figure 4c, CO₂ could be efficiently hydrogenated to CO in an atomized hexadecane-water system, and there was no apparent decline within 80 h in the consumption rate of CO₂, which could reach 0.4 mmol h⁻¹ L_{H₂O}⁻¹, with the fraction of absorbed CO₂ converted to CO reaching 92.2%. Not only the hydrocarbon-water system but also a biomass oil-water system, such as a soybean oil-water system, could be employed for CO₂ hydrogenation (Figure 4d,e). However, it was evident that at a low concentration of soybean oil, the rates of CO₂ conversion significantly declined over time. This implies that the biomass oil-water system may require a higher oil concentration to maintain the CO₂ hydrogenation activity. Although oil itself can generate CO during ultrasonic spray without CO₂ added, CO was predominantly derived from CO₂ under optimized conditions. In an ultrapure water system, the absorption of CO₂ into CO was also feasible but exhibited lower activity than that in oil-water systems (Figure 4b). The above findings indicate that the sprayed oil-water emulsion microdroplets possess superior performance for CO₂ hydrogenation relative to sprayed ultrapure water microdroplets, which is consistent with their difference in charge transfer (Figure 1c) and hydrogen evolution reactivity (Figure 3b).

The oil-water mixtures in the bulk phase are widely produced in oil spill and oily wastewater discharge, which are notorious for resulting in severe environmental contamination and substantial CO₂ emissions.^{43,44} There is an urgent need to develop green technologies for efficiently degrading or reutilizing the oil-water mixtures in order to contribute to achieving net-zero carbon emission by 2050. Currently, the most commonly used methods for oil-spill remediation and

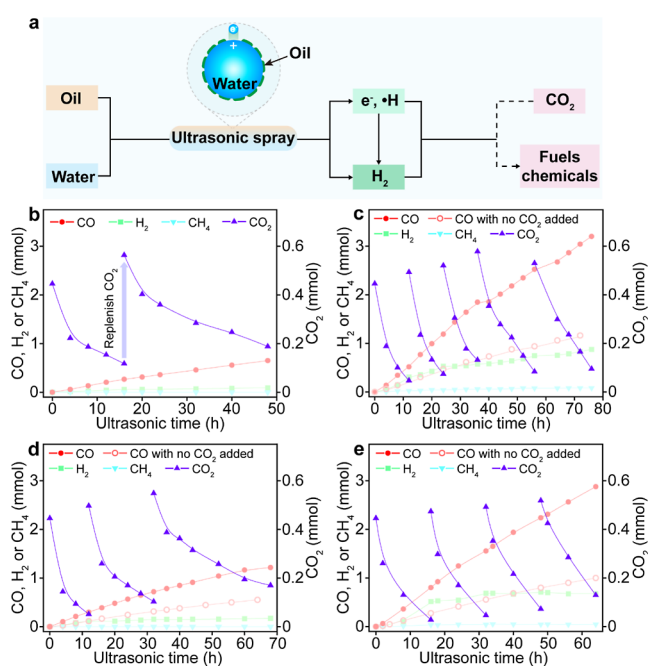


Figure 4. CO₂ hydrogenation reaction in oil–water systems. (a) Schematic overview of in situ utilization of electrons and reactive hydrogen species for CO₂ hydrogenation. Time courses of CO₂ hydrogenation in an (b) ultrapure water system (70 mL H₂O), (c) hexadecane–water system (70 mL H₂O and 0.05 mL hexadecane), (d) soybean oil–water system (70 mL H₂O and 0.05 mL soybean oil), and (e) soybean oil–water system (70 mL H₂O and 0.5 mL soybean oil).

wastewater treatment include in situ burning,⁴⁵ mechanical oil recovery,⁴⁶ and microbial degradation.⁴⁷ However, these methods inevitably lead to carbon emissions. Thus, in pursuit of carbon emission reduction and the rational utilization of emulsified oil–water mixtures, we propose the alternative of using an ultrasonic spray for the treatment of oil–water systems. As shown in Figure 4a, the sprayed oil–water microdroplets can provide in situ hydrogen species during the atomization process, enabling the hydrogenation of CO₂. By this means, oil spills and domestic wastewater can be upcycled as sources of reactive hydrogen species to provide fuels and chemicals.⁴⁸

CONCLUSIONS

In summary, our results reveal a mechanism that explains spray hydrogenation reactions that require charge separation. The charge separation of aqueous microdroplets was significantly enhanced due to the oil-mediated extraction of electrons from sprayed microdroplets. This involves contact electrification and mutual neutralization at oil–water microdroplet interfaces that facilitated the generation of hydrogen species (*H and H₂). The reductive hydrogen species could further lead to an in situ CO₂ hydrogenation process run at normal temperature for selective CO formation using water as the hydrogen source. Distinguished from solid materials having fixed shapes and volumes, breakable microdroplets provide a unique paradigm for charge separation that can be exploited for improved hydrogenation reactions. We expect that this discovery will serve to exemplify the applicability of spraying an oil–water emulsion for achieving hydrogenation or for generating H₂ from water.

ASSOCIATED CONTENT

Supporting Information

The Supporting Information is available free of charge at <https://pubs.acs.org/doi/10.1021/jacs.4c01455>.

Experimental methods, photographs and schematic of the experimental setup, particle size distribution, time courses of a H₂ product in a hexadecane–water system, mass spectrometric detection of H₂, HD, and D₂, and GC spectra supporting the data in the main text (PDF)

AUTHOR INFORMATION

Corresponding Authors

Xiuquan Jia – State Key Laboratory of Catalysis, Dalian Institute of Chemical Physics, Chinese Academy of Sciences, Dalian 116023, P. R. China; orcid.org/0000-0002-9921-234X; Email: jiaxiuquan@dicp.ac.cn

Richard N. Zare – Department of Chemistry, Stanford University, Stanford, California 94305, United States; orcid.org/0000-0001-5266-4253; Email: zare@stanford.edu

Feng Wang – State Key Laboratory of Catalysis, Dalian Institute of Chemical Physics, Chinese Academy of Sciences, Dalian 116023, P. R. China; University of Chinese Academy of Sciences, Beijing 100049, P. R. China; orcid.org/0000-0002-9167-8743; Email: wangfeng@dicp.ac.cn

Authors

Xuke Chen – State Key Laboratory of Catalysis, Dalian Institute of Chemical Physics, Chinese Academy of Sciences, Dalian 116023, P. R. China; University of Chinese Academy of Sciences, Beijing 100049, P. R. China

Yu Xia – Department of Chemistry, Stanford University, Stanford, California 94305, United States; orcid.org/0000-0001-7647-4921

Yingfeng Wu – State Key Laboratory of Catalysis, Dalian Institute of Chemical Physics, Chinese Academy of Sciences, Dalian 116023, P. R. China; Henan Institute of Advanced Technology, Zhengzhou University, Zhengzhou 450000, P. R. China

Yunpeng Xu – State Key Laboratory of Catalysis, Dalian Institute of Chemical Physics, Chinese Academy of Sciences, Dalian 116023, P. R. China

Complete contact information is available at: <https://pubs.acs.org/10.1021/jacs.4c01455>

Author Contributions

||X.C., Y.X., and Y.W. contributed equally.

Notes

The authors declare no competing financial interest.

ACKNOWLEDGMENTS

This work was supported by the National Natural Science Foundation of China (22025206 and 22172163), the Fundamental Research Funds for the Central Universities (20720220008), and the Dalian Innovation Support Plan for High Level Talents (2022RG13). R.N.Z. and Y.X. also acknowledge support from the Air Force Office of Scientific Research through the Multidisciplinary University Research Initiative program (AFOSR FA9550-21-1-0170). We thank the instrumental support of the Liaoning Key Laboratory of Biomass Conversion for Energy and Material.

REFERENCES

- (1) Catling, D. C.; Zahnle, K. J.; McKay, C. P. Biogenic methane, hydrogen escape, and the irreversible oxidation of early Earth. *Science* **2001**, *293* (5531), 839–843.
- (2) Tromp, T. K.; Shia, R.-L.; Allen, M.; Eiler, J. M.; Yung, Y. L. Potential environmental impact of a hydrogen economy on the stratosphere. *Science* **2003**, *300* (5626), 1740–1742.
- (3) Martin, W.; Müller, M. The hydrogen hypothesis for the first eukaryote. *Nature* **1998**, *392* (6671), 37–41.
- (4) McCollom, T. M.; Seewald, J. S. Serpentinites, hydrogen, and life. *Elements* **2013**, *9* (2), 129–134.
- (5) Carbonero, F.; Benefiel, A. C.; Gaskins, H. R. Contributions of the microbial hydrogen economy to colonic homeostasis. *Nat. Rev. Gastroenterol. Hepatol.* **2012**, *9* (9), 504–518.
- (6) Ohsawa, I.; Ishikawa, M.; Takahashi, K.; Watanabe, M.; Nishimaki, K.; Yamagata, K.; Katsura, K.-i.; Katayama, Y.; Asoh, S.; Ohta, S. Hydrogen acts as a therapeutic antioxidant by selectively reducing cytotoxic oxygen radicals. *Nat. Med.* **2007**, *13* (6), 688–694.
- (7) Zhang, J.; Mück-Lichtenfeld, C.; Studer, A. Photocatalytic phosphine-mediated water activation for radical hydrogenation. *Nature* **2023**, *619* (7970), 506–513.
- (8) Yoshino, S.; Takayama, T.; Yamaguchi, Y.; Iwase, A.; Kudo, A. CO₂ reduction using water as an electron donor over heterogeneous photocatalysts aiming at artificial photosynthesis. *Acc. Chem. Res.* **2022**, *55* (7), 966–977.
- (9) Lewis, N. S.; Nocera, D. G. Powering the planet: Chemical challenges in solar energy utilization. *Proc. Natl. Acad. Sci. U.S.A.* **2006**, *103* (43), 15729–15735.
- (10) Huang, R.; Xia, M.; Zhang, Y.; Guan, C.; Wei, Y.; Jiang, Z.; Li, M.; Zhao, B.; Hou, X.; Wei, Y.; Chen, Q.; Hu, J.; Cui, X.; Yu, L.; Deng, D. Acetylene hydrogenation to ethylene by water at low temperature on a Au/ α -MoC catalyst. *Nat. Catal.* **2023**, *6* (11), 1005–1015.
- (11) Adriaanse, C.; Sulpizi, M.; VandeVondele, J.; Sprik, M. The electron attachment energy of the aqueous hydroxyl radical predicted from the detachment energy of the aqueous hydroxide anion. *J. Am. Chem. Soc.* **2009**, *131* (17), 6046–6047.
- (12) Dang, L. X.; Chang, T.-M. Molecular mechanism of ion binding to the liquid/vapor interface of water. *J. Phys. Chem. B* **2002**, *106* (2), 235–238.
- (13) Xiong, H.; Lee, J. K.; Zare, R. N.; Min, W. Strong electric field observed at the interface of aqueous microdroplets. *J. Phys. Chem. Lett.* **2020**, *11* (17), 7423–7428.
- (14) Hao, H.; Leven, I.; Head-Gordon, T. Can electric fields drive chemistry for an aqueous microdroplet? *Nat. Commun.* **2022**, *13* (1), 280.
- (15) Kathmann, S. M.; Kuo, I. F. W.; Mundy, C. J. Electronic effects on the surface potential at the vapor-liquid interface of water. *J. Am. Chem. Soc.* **2009**, *131* (47), 17522.
- (16) Heindel, J. P.; Hao, H.; LaCour, R. A.; Head-Gordon, T. Spontaneous formation of hydrogen peroxide in water microdroplets. *J. Phys. Chem. Lett.* **2022**, *13* (43), 10035–10041.
- (17) Gong, C.; Li, D.; Li, X.; Zhang, D.; Xing, D.; Zhao, L.; Yuan, X.; Zhang, X. Spontaneous reduction-induced degradation of viologen compounds in water microdroplets and its inhibition by host-guest complexation. *J. Am. Chem. Soc.* **2022**, *144* (8), 3510–3516.
- (18) Chen, H.; Wang, R.; Xu, J.; Yuan, X.; Zhang, D.; Zhu, Z.; Marshall, M.; Bowen, K.; Zhang, X. Spontaneous reduction by one electron on water microdroplets facilitates direct carboxylation with CO₂. *J. Am. Chem. Soc.* **2023**, *145* (4), 2647–2652.
- (19) Yuan, X.; Zhang, D.; Liang, C.; Zhang, X. Spontaneous reduction of transition metal ions by one electron in water microdroplets and the atmospheric implications. *J. Am. Chem. Soc.* **2023**, *145* (5), 2800–2805.
- (20) Zhao, L.; Song, X.; Gong, C.; Zhang, D.; Wang, R.; Zare, R. N.; Zhang, X. Sprayed water microdroplets containing dissolved pyridine spontaneously generate pyridyl anions. *Proc. Natl. Acad. Sci. U.S.A.* **2022**, *119* (12), No. e2200991119.
- (21) Jin, S.; Chen, H.; Yuan, X.; Xing, D.; Wang, R.; Zhao, L.; Zhang, D.; Gong, C.; Zhu, C.; Gao, X.; Chen, Y.; Zhang, X. The spontaneous electron-mediated redox processes on sprayed water microdroplets. *JACS Au* **2023**, *3* (6), 1563–1571.
- (22) Song, X.; Meng, Y.; Zare, R. N. Spraying water microdroplets containing 1,2,3-triazole converts carbon dioxide into formic acid. *J. Am. Chem. Soc.* **2022**, *144* (37), 16744–16748.
- (23) Lee, J. K.; Samanta, D.; Nam, H. G.; Zare, R. N. Micrometer-sized water droplets induce spontaneous reduction. *J. Am. Chem. Soc.* **2019**, *141* (27), 10585–10589.
- (24) Song, X.; Basheer, C.; Zare, R. N. Making ammonia from nitrogen and water microdroplets. *Proc. Natl. Acad. Sci. U.S.A.* **2023**, *120* (16), No. e2301206120.
- (25) Chen, X.; Xia, Y.; Zhang, Z.; Hua, L.; Jia, X.; Wang, F.; Zare, R. N. Hydrocarbon degradation by contact with anoxic water microdroplets. *J. Am. Chem. Soc.* **2023**, *145* (39), 21538–21545.
- (26) Ju, Y.; Zhang, H.; Jiang, Y.; Wang, W.; Kan, G.; Yu, K.; Wang, X.; Liu, J.; Jiang, J. Aqueous microdroplets promote C-C bond formation and sequences in the reverse tricarboxylic acid cycle. *Nat. Ecol. Evol.* **2023**, *7* (11), 1892–1902.
- (27) Wang, S.; Shan, S.; Xiao, S.; Liu, F.; Yang, Z.; Li, S.; Qiu, Z.; Dong, X.; Cheng, Y.; Zhang, X. Spontaneously generated electrons for CO₂ hydrogenation to formate at the microinterface of air-water. *Adv. Energy Mater.* **2023**, *13*, 2303121.
- (28) Song, X.; Basheer, C.; Xia, Y.; Li, J.; Abdulazeez, I.; Al-Saadi, A. A.; Mofidfar, M.; Suliman, M. A.; Zare, R. N. One-step formation of urea from carbon dioxide and nitrogen using water microdroplets. *J. Am. Chem. Soc.* **2023**, *145* (47), 25910–25916.
- (29) Lenard, P. Ueber die electricität der wasserfälle. *Ann. Phys.* **1892**, *282* (8), 584–636.
- (30) Tammet, H.; Hörrak, U.; Kulmala, M. Negatively charged nanoparticles produced by splashing of water. *Atmos. Chem. Phys.* **2009**, *9* (2), 357–367.
- (31) Lin, S.; Cao, L. N. Y.; Tang, Z.; Wang, Z. L. Size-dependent charge transfer between water microdroplets. *Proc. Natl. Acad. Sci. U.S.A.* **2023**, *120* (31), No. e2307977120.
- (32) Burgo, T. A. L.; Galembeck, F. On the spontaneous electric-bipolar nature of aerosols formed by mechanical disruption of liquids. *Colloid Interface Sci. Commun.* **2015**, *7*, 7–11.
- (33) Bogot, A.; Poline, M.; Ji, M.; Dochain, A.; Simonsson, A.; Rosén, S.; Zettergren, H.; Schmidt, H. T.; Thomas, R. D.; Strasser, D. The mutual neutralization of hydronium and hydroxide. *Science* **2024**, *383* (6680), 285–289.
- (34) Plastring, B.; Cohen, M. H.; Cowen, K. A.; Wood, D. A.; Coe, J. V. Effect of clustering on mutual neutralization rates using electrostatically merged ion beams: H₃O⁺(H₂O)_{n=0–3} + OH⁻(H₂O)_{m=0–3}. *J. Phys. Chem.* **1995**, *99* (1), 118–122.
- (35) Pezzotti, S.; Serva, A.; Gaigeot, M.-P. 2D-HB-Network at the air-water interface: A structural and dynamical characterization by means of ab initio and classical molecular dynamics simulations. *J. Chem. Phys.* **2018**, *148* (17), 174701.
- (36) Pullanchery, S.; Kulik, S.; Rehl, B.; Hassanali, A.; Roke, S. Charge transfer across C–H···O hydrogen bonds stabilizes oil droplets in water. *Science* **2021**, *374* (6573), 1366–1370.
- (37) Ge, Q.; Liu, Y.; Li, K.; Xie, L.; Ruan, X.; Wang, W.; Wang, L.; Wang, T.; You, W.; Zhang, L. Significant acceleration of photocatalytic CO₂ reduction at the gas-liquid interface of microdroplets. *Angew. Chem., Int. Ed.* **2023**, *62*, No. e202304189.
- (38) Li, K.; Ge, Q.; Liu, Y.; Wang, L.; Gong, K.; Liu, J.; Xie, L.; Wang, W.; Ruan, X.; Zhang, L. Highly efficient photocatalytic H₂O₂ production in microdroplets: accelerated charge separation and transfer at interfaces. *Energy Environ. Sci.* **2023**, *16* (3), 1135–1145.
- (39) Chamberlayne, C. F.; Zare, R. N. Microdroplets can act as electrochemical cells. *J. Chem. Phys.* **2022**, *156*, 054705.
- (40) Gong, K.; Ao, J.; Li, K.; Liu, L.; Liu, Y.; Xu, G.; Wang, T.; Cheng, H.; Wang, Z.; Zhang, X.; Wei, H.; George, C.; Mellouki, A.; Herrmann, H.; Wang, L.; Chen, J.; Ji, M.; Zhang, L.; Francisco, J. S. Imaging of pH distribution inside individual microdroplet by

stimulated Raman microscopy. *Proc. Natl. Acad. Sci. U.S.A.* **2023**, *120* (20), No. e2219588120.

(41) Liu, Y.; Ge, Q.; Wang, T.; Zhang, R.; Li, K.; Gong, K.; Xie, L.; Wang, W.; Wang, L.; You, W.; Ruan, X.; Shi, Z.; Han, J.; Wang, R.; Fu, H.; Chen, J.; Chan, C. K.; Zhang, L. Strong electric field force at the air/water interface drives fast sulfate production in the atmosphere. *Chem* **2024**, *10* (1), 330–351.

(42) Bai, C.; Herzfeld, J. Special pairs are decisive in the autoionization and recombination of water. *J. Phys. Chem. B* **2017**, *121* (16), 4213–4219.

(43) Freeman, D. H.; Ward, C. P. Sunlight-driven dissolution is a major fate of oil at sea. *Sci. Adv.* **2022**, *8* (7), No. eabl7605.

(44) Li, L.; Wang, X.; Miao, J.; Abulimiti, A.; Jing, X.; Ren, N. Carbon neutrality of wastewater treatment-A systematic concept beyond the plant boundary. *Environ. Sci. Ecotech.* **2022**, *11*, 100180.

(45) Fritt-Rasmussen, J.; Wegeberg, S.; Lassen, P.; Wilms, L. B.; Renvald, L.; Larsen, M. B.; Geertz-Hansen, O.; Wiktor, J.; Gustavson, K. Coastline in-situ burning of oil spills, analysis of a Greenland field experiment. *J. Hazard. Mater.* **2023**, *441*, 129976.

(46) Liu, B.; Chen, B.; Ling, J.; Matchinski, E. J.; Dong, G.; Ye, X.; Wu, F.; Shen, W.; Liu, L.; Lee, K.; Isaacman, L.; Potter, S.; Hynes, B.; Zhang, B. Development of advanced oil/water separation technologies to enhance the effectiveness of mechanical oil recovery operations at sea: Potential and challenges. *J. Hazard. Mater.* **2022**, *437*, 129340.

(47) Pyke, R.; Fortin, N.; Wasserscheid, J.; Tremblay, J.; Schreiber, L.; Levesque, M.-J.; Messina-Pacheco, S.; Whyte, L.; Wang, F.; Lee, K.; Cooper, D.; Greer, C. W. Biodegradation potential of residue generated during the in-situ burning of oil in the marine environment. *J. Hazard. Mater.* **2023**, *445*, 130439.

(48) Xu, J.; Wang, J.; Ma, C.; Wei, Z.; Zhai, Y.; Tian, N.; Zhu, Z.; Xue, M.; Li, D. Embracing a low-carbon future by the production and marketing of C1 gas protein. *Biotechnol. Adv.* **2023**, *63*, 108096.